Central European Journal of Energetic Materials
ISSN 1733-7178; e-ISSN 2353-1843

Cent. Eur. J. Energ. Mater. 2019, *16*(3): 433-448; DOI 10.22211/cejem/112268
Article is available in PDF-format, in colour, at:
http://www.wydawnictwa.ipo.waw.pl/cejem/Vol-16-Number3-2019/CEJEM_01067.pdf

Research paper

On a Certain Method of Determining the Burning Rate of Gun Propellant

Zbigniew Leciejewski,* Zbigniew Surma

Military University of Technology, Faculty of Mechatronics and Aerospace, Institute of Armament Technology, gen. S. Kaliskiego 2 Street, 00-908 Warsaw, Poland
**E-mail:* zbigniew.leciejewski@wat.edu.pl

Abstract: The relation between the burning rate, r, of a solid propellant and the pressure, p, of gases surrounding the burning propellant surface is the basic component of the gas inflow equation. The applicability of a linear form of the burning rate law is limited only to those propellants for which the same pressure impulses, I_p, were obtained during closed vessel tests at different loading densities. To determine the values of the power form of the burning rate law it is necessary to know the values of the energetic and ballistic characteristics of the propellant. In this paper, a method is presented for determining the relation $r(p)$ for which the only input data are the pressure, $p(t)$, of the propellant gases recorded during closed vessel tests (only for a single specific loading density) and information on the shape and geometric dimensions of the propellant grains. An analysis of the possibility of applying the proposed method, through examples of single-base, double-base and multi-base propellants with neutral and progressive characteristics of burning surface changes, was carried out for the purposes of the present study. The qualitative and quantitative results of burning rate analyses prove the validity of the assumptions made.

Keywords: ballistics, closed vessel test, gun propellant, burning rate

1 Introduction

The simulation of the shot phenomenon in a barrel propulsion system enables the determination of the ballistic curve, $p(t)$, which represents the changes in pressure, p, of the propellant gases *versus* time, t, in the space behind the shell. The qualitative and quantitative nature of the $p(t)$ curve affects the velocity, V_p, of the projectile in the barrel or at a certain distance from the barrel muzzle. In ballistic analyses, the value characterising the dynamics of the propellant burning process (dynamics of the change in the propellant gas pressure, p, *versus* time, t) is the relation between its burning rate, r, and pressure, p, of the gases surrounding the burning propellant surface, and is defined as the burning rate law. Assuming that the grains contained in the propellant charge:

– are chemically and physically homogeneous;
– are uniform in shape and dimensions (including the flammable layer thickness, e_1);
– ignite immediately over their entire surface and burn in such a manner that the front of the flame moves in parallel layers into the grain, and at each point on the surface, S, the grains burn at the same temporary rate, r, depending on the pressure, p, [1-4].

In principle, two forms of the burning rate law – namely the linear form and the power form – are considered. The linear burning rate law is known as the following Equation 1:

$$r(p) = \frac{de}{dt} = r_1 \cdot p \tag{1}$$

where coefficient r_1 depends on the physico-chemical properties and initial temperature of the propellant. The value of coefficient r_1 (assumed as constant for a given propellant and for its entire burning process) is determined from the following Equation 2 [2]:

$$r_1 = \frac{e_1}{\int_0^{t_k} p dt} = \frac{e_1}{I_p} \tag{2}$$

The basis for its determination is a knowledge of the value of the thickness of the combustible layer, e_1, of the grain of the tested propellant, and of the value of the total pressure impulse, I_p, *i.e.* the integral of the pressure, $p(t)$, of propellant gases recorded during closed vessel tests, which results from the burning of the tested propellant (measured within the limits defined by the ignition time and the time when the burning of the propellant ended, t_k). According to [2], the applicability of this form of the burning rate law is limited; however, it is limited only to those propellants for which the same pressure impulses were obtained during closed vessel tests at different loading densities. Moreover, the values of coefficient r_1 for a specific type of propellant may contain significant errors resulting from differences in the determination of the flammable layer thickness of the propellant grains, particularly with regard to fine-grained propellants [5, 6] and to the ignition system used [7].

The most common form of the burning rate law, which is employed in the research of various laboratories, is the power form of the burning rate, $r(p)$, [1, 3], known as Saint Robert's equation (Equation 3):

$$r(p) = \frac{de}{dt} = \beta \cdot p^{\alpha} \tag{3}$$

where β and α are the coefficient and the exponent of the power form of the burning rate, respectively. In Equation 3, the power coefficient and the exponent are constants that characterise a given propellant composition.

For this form of the burning rate law, the aforementioned limitations formulated for the linear form of the burning rate law do not apply. The determination of the burn rate, $r(p)$, followed by coefficient β and exponent α, is possible in this case by comparing the two forms of the gas inflow equation [2, 8]; resulting from the analysis of the geometric model of propellant burning (Equation 4):

$$\frac{dz}{dt} = \frac{S_1}{\Lambda_1} \cdot \Phi \cdot r(p) \tag{4}$$

in which the relative mass burning rate of the propellant charge, dz/dt, is dependent on:

- the initial geometric dimensions of the propellant grains (allowing their initial values of the burning surface, S_1, and volume, Λ_1, to be determined);
- the function of the grain burning-surface change, Φ, during the burning process; and
- the burning rate, $r(p)$, as a function of p, the propellant gas pressure.

The argument of function Φ can be a relative part of a burnt propellant grain mass, z, or the ratio of the current thickness of the burnt propellant grain layer, e, to the thickness of the combustible layer, e_1, and it is expressed as:

$$\frac{dz}{dt} = \frac{dz}{dp} \cdot \frac{dp}{dt} \tag{5}$$

where the value of *dz*/*dp* results from the equation of pyrostatics:

$$\frac{dz}{dp} = \frac{1}{p_{max}} \cdot \frac{1 + \left(\eta - \frac{1}{\delta}\right) \cdot \frac{p_{max}}{f}}{\left[1 + \left(\eta - \frac{1}{\delta}\right) \cdot \frac{p}{f}\right]^2} \tag{6}$$

As a result of the comparison of Equations 4 and 5 of the gas inflow, a burning rate equation is obtained in the following form:

$$r(p) = \frac{dp}{dt} \cdot \frac{\Lambda_1}{S_1 \cdot \Phi} \cdot \frac{1}{p_{max}} \cdot \frac{1 + \left(\eta - \frac{1}{\delta}\right) \cdot \frac{p_{max}}{f}}{\left[1 + \left(\eta - \frac{1}{\delta}\right) \cdot \frac{p}{f}\right]^2} \tag{7}$$

An analysis of the above equation shows that to determine the burning rate, it is necessary to know the shape and the geometric dimensions of the propellant grains, the coefficients of the Noble-Abel gas equation of state (specific force, f, and co-volume, η) – which can be obtained both from pyrostatic tests and thermochemical calculations – as well as the $p_{\max}$ and $p(t)$ values recorded during the experimental tests.

Equation 7 is a development of the burning rate equation defined in the NATO Standardisation Agreement [9] as:

$$r(p) = \frac{dp}{dt} \cdot \frac{de}{dz} \cdot \frac{dz}{dp} \tag{8}$$

for which the input data are the following elements:

– *dp*/*dt* – resulting from the development of the experimental curve, $p(t)$;
– *dz*/*dp* – defined by Equation 6,
– *de*/*dz* – resulting from the analysis of the thickness change in the burnt propellant grain layer depending on the relative change in the mass of the burnt propellant grain using the geometric burning model:

$$\frac{de}{dz} = \frac{\Lambda_1}{S_1} \cdot \frac{1}{\Phi} \tag{9}$$

The aim of this study was to analyse the possibility of proposing a relation which allows the rate of propellant burning (where the shape and dimensions of the propellant grains are known) to be determined, for which the values of the energetic and ballistic characteristics (coefficients of the propellant-gas state equation: specific force, f, and co-volume, η) have not been determined or are not known.

2 Description of the Test Method and Test Material

Using the equation of Noble-Abel for the case of the total propellant burning:

$$p_{max} = \frac{f \cdot \Delta}{1 - \eta \cdot \Delta}, \tag{10}$$

Equation 7 can be brought to the following form [2, 8]:

$$r(p) = \frac{dp}{dt} \cdot \frac{\Lambda_1}{\cdot S_1 \cdot \Phi} \cdot \frac{1}{p_{max}} \cdot \frac{\left(1 - \frac{\Delta}{\delta}\right) \cdot (1 - \eta\Delta)}{\left[(1 - \eta\Delta) + \frac{p}{p_{max}} \cdot \left(\eta\Delta - \frac{\Delta}{\delta}\right)\right]^2} \tag{11}$$

where the specific force, f, no longer exists and the rate of burning of the propellant charge, $r(p)$, depends on:

- a knowledge of the shape and of the geometric dimensions of the propellant grains;
- the loading density, Δ;
- the propellant density, δ;
- the p_{max} values and changes in $p(t)$ recorded during the closed vessel tests; and
- the co-volume, η, of the propellant gases, which occurs in the last factor of the right-hand side of Equation 11, designated for further analysis as Y:

$$Y = \frac{\left(1 - \frac{\Delta}{\delta}\right) \cdot (1 - \eta\Delta)}{\left[(1 - \eta\Delta) + \frac{p}{p_{max}} \cdot \left(\eta\Delta - \frac{\Delta}{\delta}\right)\right]^2} \tag{12}$$

Therefore, to eliminate the relation of the burning rate, $r(p)$, on the propellant gas co-volume η, further consideration was given to the possibility of replacing the variable value of parameter Y (Equation 12) with its average value, which could be determined on the basis of an analysis of the results of closed vessel studies of propellants with known energetic and ballistic parameters.

The validity of such an approach was tested by comparing the burning rate determined on the basis of Equations 7 and 11 with previously described conditions. For this purpose, closed vessel tests were conducted, in which the following gun propellants were tested:

(a) a single-base 4/1 propellant with cylindrical grain and a central channel (one-perforated grain),
(b) a double-base JA-2 propellant with seven-perforated grains LO5460, and
(c) a Polish multi-base low-sensitivity propellant, namely SC92, with seven-perforated grains.

The JA-2 propellant and its modifications are used in tank ammunition [10-12]; the 4/1 propellant is used in small- and medium-calibre Polish ammunition, whereas the SC92 propellant is a newly developed propellant intended for Polish tank ammunition. The dimensions and values of the shape coefficients of the analysed propellants are listed in Table 1.

Table 1. Dimensions and shape coefficients (χ, λ, μ) of LO5460 grains of the JA-2 propellant and grains of the 4/1 and SC92 propellants

Parameter	SB 4/1	DB JA-2 (LO5460)	MB SC92
Grain shape	cylindrical		
Number of channels	1	7	
Grain length, L [mm]	6.2	15.5	5.0
Grain diameter, D [mm]	0.99	8.9	9.0
Channel diameter, d [mm]	0.25	0.546	0.5
Flammable layer thickness, e_1 [mm]	0.185	0.91	0.938
Grain volume, Λ_1 [cm^3]	0.00447	0.939	0.311
Grain surface area, S_1 [cm^2]	0.256	7.38	3.21
Λ_1/S_1 [cm]	0.0175	0.127	0.097
χ	1.0597	0.716	0.967
λ	–0.0563	0.262	0.0459
μ	0	–0.0423	–0.1033

Closed vessel tests of the aforementioned propellants were conducted in the Ballistics Laboratory of the Institute of Armament Technology, Military University of Technology (Warsaw, Poland) with the use of a pressure chamber with a volume of W_0 = 200 cm^3. Black powder-based primers were used to ignite the tested propellant charges. The primer mass was selected to be such that the conventional ignition pressure value would be 3 MPa. The results of the closed vessel tests were the values of the propellant gas pressure *versus* time, $p(t)$, for two loading densities, namely 100 and 200 kg/m^3.

3 Test Results and Discussion

The determination of the burning rate, $r(p)$, for a propellant of known shape and of known grain dimensions based on Equation 7 requires *prior* knowledge of the values of the coefficients of the Noble-Abel equation (specific force, f, and co-volume, η). On the basis of the recorded values of the maximum pressure, p_{max_E}, (for two loading densities: Δ_1 = 100 and Δ_2 = 200 kg/m^3) the values of the coefficients of the Noble-Abel gas state equation, the specific force, f_E, and the co-volume, η_E, were determined as:

$$f_E = \frac{p_{max1\_E}}{\Delta_1} \cdot \frac{p_{max2\_E}}{\Delta_2} \cdot \frac{\Delta_1 - \Delta_2}{p_{max1\_E} - p_{max2\_E}} \tag{13}$$

$$\eta_E = \frac{\frac{p_{max2\_E}}{\Delta_2} - \frac{p_{max1\_E}}{\Delta_1}}{p_{max2\_E} - p_{max1\_E}} \tag{14}$$

During the burning of the propellant charge in the pressure chamber (closed vessel test), the propellant gases heated up the walls of the chamber; consequently, their internal energy and temperature decreased [2, 3, 13-16]. In addition, during the pressure measurement, discharge of the piezoelectric sensor occurs. The quantitative effect of these processes is a decrease in both the propellant-gas current pressure and the maximum pressure, p_{max}, at the instant when the complete burning of the tested propellant charge has been achieved. Based on [13, 15], the differences were determined between the pressure that would be measured in the absence of losses and the recorded pressure; subsequently, the current pressure *versus* time, $p(t)_{EQ}$, (and of course the maximum pressure, p_{max_EQ}), corrected for heat loss and sensor discharge, was determined [17] as:

$$p(t)_{EQ} = p(t)_E + \frac{p_{\max\_E} - p_{ign}}{t_h} \cdot t + \frac{1}{t_q}\int_0^t p_E dt \tag{15}$$

where p_{ign} – ignition pressure; t_h, t_q – time constant of heat losses and time constant of the piezoelectric transducer discharge, respectively; determined on the basis of the falling part (after maximum pressure, p_{max_E}) of the pressure curve [17].

The values of the corrected maximum pressure considering the previously described losses were the basis for the determination (according to Equations 13 and 14) of the specific force, f_Q, and the co-volume, η_Q. The calculated values of the specific force and the co-volume are listed in Table 2.

Table 2. Values of specific force, *f*, and co-volume, η: experimental (E index) and corrected for heat loss and sensor discharge (Q index)

Propellant	Specific force [kJ/kg]		co-volume [dm^3/kg]	
	f_E	f_Q	η_E	η_Q
SB 4/1	953.8	992.0	1.339	1.217
DB JA-2 (LO5460)	1020	1153	1.359	1.001
MB SC92	989	1153	1.530	1.103

The calculated values of specific force, *f*, and co-volume, η, as well as the recorded and corrected values of pressure *versus* time, $p(t)$, were the basis for determining the $Y(p/p_{max})$ function for the analysed propellants. Diagrams of $Y(p/p_{max})$ functions at a loading density $\Delta = 200$ kg/m^3, for data acquired:

– directly from the experimental tests (method E), and
– including heat loss and sensor discharge (method Q),

are shown in Figures 1-3.

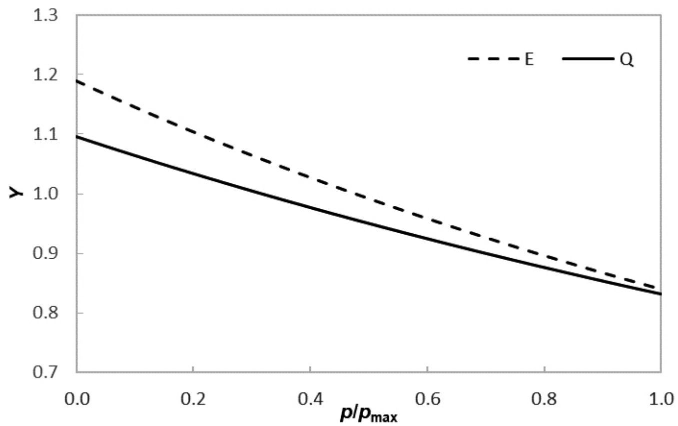

Figure 1. $Y(p/p_{max})$ diagrams for 4/1 propellant for methods E and Q

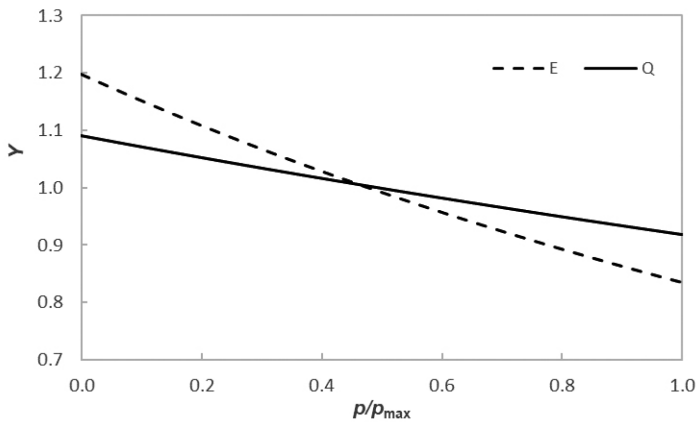

Figure 2. $Y(p/p_{max})$ diagrams for JA-2 propellant for methods E and Q

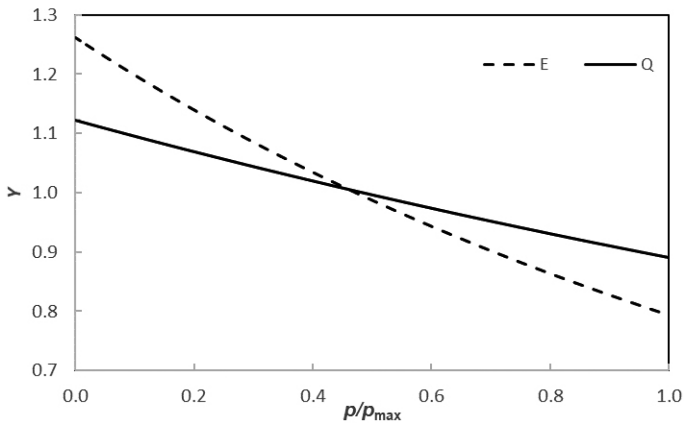

Figure 3. $Y(p/p_{max})$ diagrams for SC92 propellant for methods E and Q

Comparing the $Y(p/p_{max})$ diagrams, it may be noticed that the Y function:

– for method E changes regularly from > 1 at the start of burning to < 1 at the end of burning (Table 3),

Table 3. Values of the Y function for the start and end of burning (method E)

Propellant	SB 4/1	DB JA-2 (LO5460)	MB SC92
Y (p/p_{max} = 0)	1.189	1.197	1.261
Y (p/p_{max} =1)	0.841	0.835	0.793

– after considering the thermal losses and the sensor discharge (method Q), reduces the difference between the initial and final value (Table 4).

Table 4. Values of the Y function for the start and end of burning (method Q)

Propellant	SB 4/1	DB JA-2 (LO5460)	MB SC92
Y (p/p_{max} = 0)	1.095	1.085	1.123
Y (p/p_{max} =1)	0.832	0.922	0.891

Taking into account the considerations and analyses which have been carried out, the burning rate *versus* the gas pressure was determined on the basis of Equation 7 and on the basis of the following Equation 16:

$$r(p) = \frac{dp}{dt} \cdot \frac{\Lambda_1}{\cdot S_1 \cdot \Phi} \cdot \frac{1}{p_{max}} \tag{16}$$

resulting from Equation 11, in which it is assumed that $Y = 1$. The relative burning surface area, Φ, of the propellant grains was calculated as in the following Equation 17:

$$\Phi = 1 + 2 \cdot \lambda \cdot \varepsilon + 3 \cdot \mu \cdot \varepsilon^2 \tag{17}$$

in which λ and μ are the shape coefficients of the propellant grains and ε expresses the ratio of the current thickness of the burnt grain propellant layer, e, to the thickness of the combustible layer, e_1, the value of which is proposed to be calculated from the ratio of the current value of the pressure impulse, I_c, to the value of the total pressure impulse, I_p:

$$\varepsilon = \frac{e}{e_1} = \frac{I_c}{I_p} \tag{18}$$

Figures 4-6 present the $r(p)$ diagrams for the analysed propellants, which were obtained on the basis of Equation 7 and of the data obtained *via* the method described as Q, and on the basis of Equation 16 for which only the shape and dimensions of the propellant grains, as well as the experimental diagram of $p(t)$ are the input data.

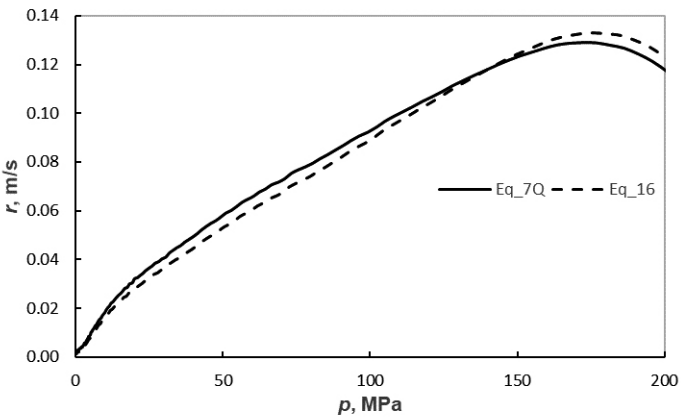

Figure 4. Diagrams $r(p)$ for the 4/1 propellant plotted on the basis of Equations 7 (method Q) and 16

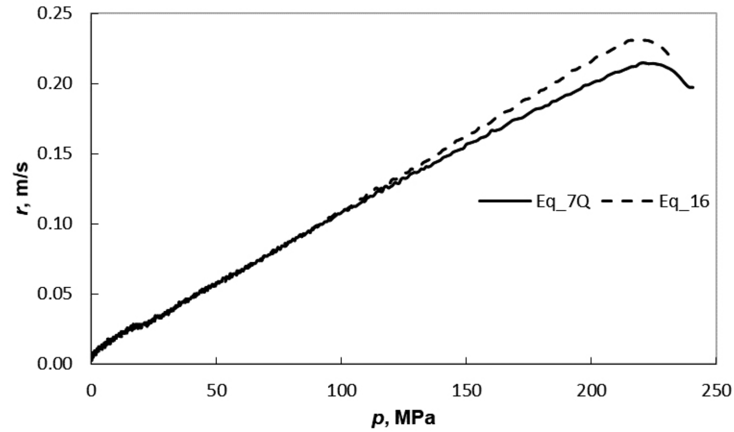

Figure 5. Diagrams $r(p)$ for the JA-2 propellant plotted on the basis of Equations 7 (method Q) and 16

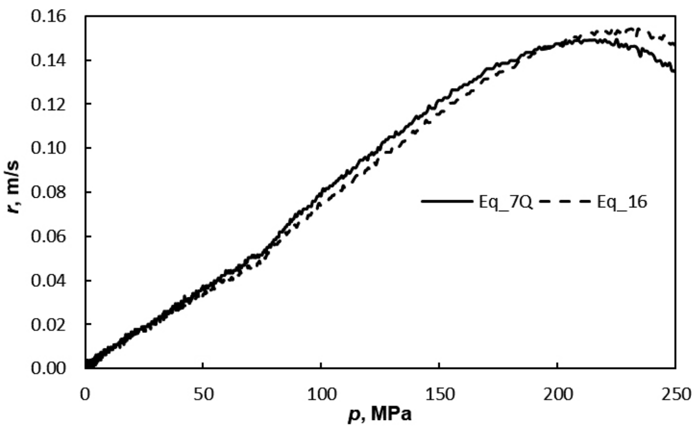

Figure 6. Diagrams $r(p)$ for the SC92 propellant plotted on the basis of Equations 7 (method Q) and 16

The relative percentage differences in burning rate (RD_{br}) between the burning rate determined from Equation 16 and that determined from Equation 7 for the method Q as:

$$RD_{br} = \frac{r_{(Eq.16)} - r_{(Eq.7Q)}}{r_{(Eq.7Q)}} \cdot 100 \tag{19}$$

for the analysed propellants are shown in the Figures 7-9. The analysis of the RD_{br} value has been limited to the range from 0.3 to 0.7 p/p_{max} according to [9]. In this way, the initial firing-up period of the propellant grains and the final combustion period were eliminated from the analyses. In real conditions, in these periods the assumptions of the combustion model described in the introduction may not work.

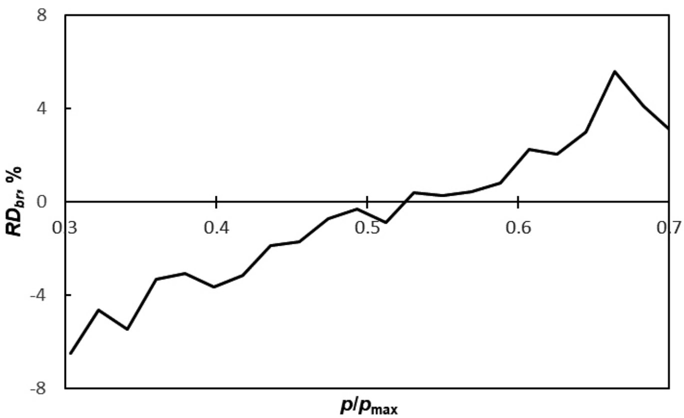

Figure 7. Relative difference in burning rate for the 4/1 propellant

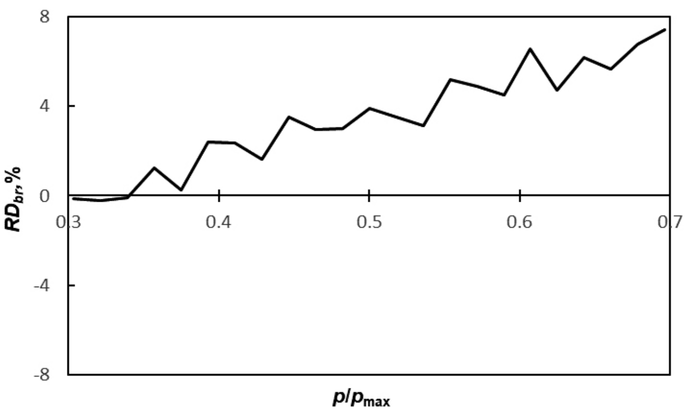

Figure 8. Relative difference in burning rate for the JA-2 propellant

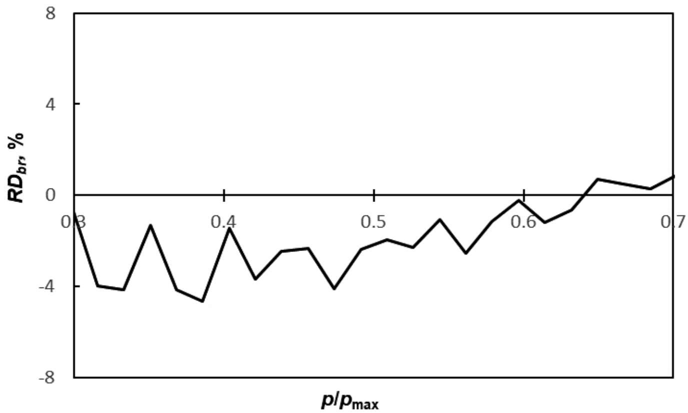

Figure 9. Relative difference in burning rate for the SC92 propellant

An analysis of the $r(p)$ diagrams developed on the basis of Equation 7 and the analysis of those developed on the basis of Equation 16 shows that they are comparable qualitatively (Figures 4-6) and quantitatively (Figures 7-9), which proves the validity of the assumptions made to determine the propellant burning rate only on the basis of prior knowledge of the geometric dimensions of the propellant grains and of the discrete values, $p(t)$, recorded during closed vessel tests.

The burning rate determined on the basis of Equation 16, just like the one determined on the basis of Equation 7, can be used to simulate the phenomenon of a shot [18]. In both cases, the correction of the burning rate is predicted by applying a fitting factor, f_β (burning rate factor).

4 Conclusions

In this paper, we present considerations on a method of determining the rate of burning, $r(p)$, of a solid propellant only on the basis of pressure $p(t)$, which had been recorded during closed vessel tests (for a specific loading density), and a knowledge of the shape and geometric dimensions of the propellant grains. This method does not require *prior* knowledge of the values of the energetic and ballistic characteristics (in the form of specific force and co-volume) of the propellant. However, it should be noted that such an approach was applicable only under the assumption that parameter Y = 1 and that the relative burning area, Φ, with the propellant-grain method was calculated *via* Equation 17 while considering the condition described in Equation 18. The proposed method was verified on the following examples: a 4/1 single-base propellant with cylindrical single-perforated grains and the JA-2 double-base propellant with seven-perforated grains, *i.e.* the LO5460 and SC92 multi-base low-sensitivity propellant. The diagrams presented in Figures 4-9 show that the $r(p)$ trends obtained from Equations 7 and 16 are comparable, both in terms of quality and quantity.

To determine the absolute burning rate, appropriate analyses must be performed considering the thermal losses to allow an appropriate correction of both the maximum pressure of the propellant gases and the discrete pressure values during the burning of the propellant under pyrostatic conditions.

Equation 11 transformed into the following form (under the assumption that $Y = 1$ and after dividing the left and right sides by pressure p):

$$\frac{1}{p} \cdot \frac{S_1}{\Lambda_1} \cdot \Phi \cdot r(p) = \frac{dp}{dt} \cdot \frac{1}{p \cdot p_{max}} \tag{20}$$

provides the possibility to compare the gas inflow intensity, Γ (left side of the above Equation 20), defined in [2] as a dynamic vivacity, L (right side of the Equation 20) defined in [9], only under the condition that discrete r-values corresponding to the current pressure, p, are introduced.

Funding
This work was supported by the Polish National Research Centre [grant DOB-BIO8/05/01/2016].

References

[1] Corner, J. *Theory of the Interior Ballistics of Guns.* John Wiley and Sons, New York, **1950**.
[2] Sieriebriakov, M. *Internal Ballistics.* (in Polish) Publishing House of Polish MoD, Warsaw, **1955**.
[3] Krier, H.; Summerfield, M. *Interior Ballistic of Guns. Progress in Astronautics and Aeronautics – Vol. 66*, American Institute of Aeronautics and Astronautics, New York, **1979**.
[4] Carlucci, D.E; Jacobson, S.S. *Ballistics: Theory and Design of Guns and Ammunition.* 2nd ed., CRC Press, Taylor and Francis Group, Boca Raton, **2014**; ISBN-13 978-1-4665-6439-8.

[5] Leciejewski, Z. Experimental Study of Possibilities for Employment of Linear Form of Burning Rate Law to Characterise the Burning Process of Fine-Grained Propellants. *Cent. Eur. J. Energ. Mater.* **2008**, *5*(1): 45-61.

[6] Pocock, M.D.; Locking, P.M.; Guyott, C.C. Effect of Statistical Variation in *Grain Geometry on* Internal Ballistics Modelling. *Int. Symp. Ballistics*, *Proc., 21st,* Adelaide, Australia, **2004**, 610-615.

[7] Leciejewski, Z.; Surma, Z. Effect of Application of Various Ignition Conditions in Closed-Vessel Tests on Burning Rate Calculation of a Fine-Grained Propellant. *Combust. Explos. Shock Waves* **2011**, *47*(2): 209-216.

[8] Oberle, F.W. *Dynamic Vivacity and Its Application to Conventional and Electrothermal-Chemical (ETC) Closed Chamber Results*. ARL-TR-2631 Report, **2001**.

[9] STANAG 4115 Land (Edition 2): *Definition and Determination of Ballistic Properties of Gun Propellants.* Military Agency for Standardization, Brussels, **1997**.

[10] Manning, G.T.; Leone, J.; Zebregs, M.; Ramlal, R.D.; van Driel, A.Ch. Definition of a JA-2 Equivalent Propellant to be Produced by Continuous Solventless Extrusion. *J. Appl. Mech.* **2013**, *80*: 031405-1-7.

[11] Conner, C.B.; Anderson, W.R. Modelling the Combustion of JA2 and *Solid Propellants of* Similar Composition. *Proc. Combust. Inst.* **2009**, 2131-2137.

[12] Heil, M.; Bohn, M.A. Long Term Mass Loss Studies of Propellants Used in Ageing Analysis. *Int. NC-Symp., Presentation, 7th,* Montreal, Canada, **2016**.

[13] Torecki, S. Experimental Estimation of the Influence of Heat Losses on the *Pressure of* Propellant Gases in Closed Vessel. (in Polish), *Sci. Aspects Armament Technol., Int. Conf., Proc., 2nd,* Waplewo, Poland **1998**, 333-341.

[14] Homan, B.E.; Juhasz, A.A. *A New Closed-Bomb Data Acquisition and Reduction Program*. ARL-TR-2491 Report, **2001**.

[15] Khomenko, Y.P.; Shirokov, V.M. Determining the Unsteady Combustion Behavior of Propellants from Results of Closed-Bomb Testing. *Combust. Explos. Shock Waves* **2006**, *42*(2): 149-157.

[16] Chereches, T.; Gheorghian, S. Determination of the Maximum Errors of the Force and Gas Covolume of a Propellant Estimated from Closed Bomb Experiment. *Armament'2007, Sci. Conf., Proc., 17th*, Rynia, Poland, **2007**, 47-50.

[17] Trębiński, R.; Surma, Z.; Leciejewski, Z.; Fikus, B. Some Considerations on the *Methods of Analysis of Closed* Vessel Test Data. *Int. Symp. Ballistics*, *Proc., 29th,* Edinburgh, Scotland, UK, **2016**, 607-617.

[18] STANAG 4367 Land (Edition 2): *Thermodynamic Interior Ballistic Model with Global Parameters.* Military Agency for Standardization, Brussels, **2000**.

Received: May 13, 2019
Revised: September 11, 2019
First published online: September 20, 2019